

Advanced Composite High- κ Gate Stack for Mixed Anion Arsenide-Antimonide Quantum Well Transistors

A. Ali, H. Madan, R. Misra, E. Hwang, A. Agrawal, I. Ramirez, P. Schiffer, T. N. Jackson, S. E. Mohny, J. B. Boos¹, B. R. Bennett¹, I. Geppert², M. Eizenberg² and S. Datta

Penn State University, University Park, PA, USA;

¹Naval Research Lab, Washington, DC, USA; ²Technion - Israel Institute of Technology University, Haifa, Israel;

Tel: (814) 865-0519, Fax: (814) 865-7065, Email: aual76@psu.edu

Abstract

This paper demonstrates the integration of a composite high- κ gate stack (3.3 nm Al_2O_3 -1.0 nm GaSb) with a mixed anion $\text{InAs}_{0.8}\text{Sb}_{0.2}$ quantum-well field effect transistor (QWFET). The composite gate stack achieves; (i) EOT of 4.2 nm with $<10^{-7}\text{A}/\text{cm}^2$ gate leakage (ii) low D_{it} interface ($\sim 1 \times 10^{12}/\text{cm}^2/\text{eV}$) (iii) high drift μ of 3,900-5,060 $\text{cm}^2/\text{V-s}$ at N_s of 5×10^{11} - $3 \times 10^{12}/\text{cm}^2$. The $\text{InAs}_{0.8}\text{Sb}_{0.2}$ MOS-QWFETs with composite gate stack exhibit extrinsic (intrinsic) g_m of 334 (502) $\mu\text{S}/\mu\text{m}$ and drive current of 380 $\mu\text{A}/\mu\text{m}$ at $V_{DS} = 0.5\text{V}$ for $L_g = 1\mu\text{m}$.

Introduction

Mixed anion $\text{InAs}_y\text{Sb}_{1-y}$ quantum-wells (QW) with high electron mobility are candidates for integration with high hole mobility $\text{In}_x\text{Ga}_{1-x}\text{Sb}$ QW for ultra-low power complementary applications¹. With the exception of a recent $\text{In}_{0.7}\text{Ga}_{0.3}\text{As}$ QWFET with high- κ gate stack², nearly all QWFETs, reported to date, use Schottky gates and suffer from high gate leakage. For further scaling, a gate stack is needed for integration with $\text{InAs}_y\text{Sb}_{1-y}$ QWFET, with low EOT and J_{OX} , good interface properties and high carrier mobility in the channel. Here, we integrate a composite high- κ gate stack (Al_2O_3 -GaSb) with $\text{InAs}_{0.8}\text{Sb}_{0.2}$ QWFET, resulting in high performance transistors operating at 0.5V V_{DS} .

Materials Characterization

MBE grown mixed anion $\text{InAs}_y\text{Sb}_{1-y}$ QW exhibit room temperature electron mobility between 11,000-22,000 $\text{cm}^2/\text{V-s}$ with varying electron density³, corresponding to ballistic mean free path of $\sim 400\text{nm}$, making them promising channel material candidates for high-speed, low power electronics (Fig. 1). To retain the high carrier mobility in $\text{InAs}_{0.8}\text{Sb}_{0.2}$ QWFET, the high- κ dielectric is deposited on the upper barrier and not directly on the channel. We incorporated an ultra-thin (1nm) GaSb layer in the upper barrier as it avoids Al at the interface and associated surface oxidation. Using n-type and p-type GaSb(100) MOS capacitors, we evaluated both ALD and Plasma Enhanced ALD (PEALD) Al_2O_3 dielectrics and confirmed unpinning Fermi level in GaSb MOS system with the latter (Fig. 2a)⁴. By minimizing elemental Sb at the GaSb/ Al_2O_3 interface using the low temperature PEALD Al_2O_3 , we demonstrate low D_{it} ($\sim 1 \times 10^{12}/\text{cm}^2/\text{eV}$) near the valence band making the composite 3.3nm Al_2O_3 /1nm GaSb gate stack suitable for $\text{InAs}_{0.8}\text{Sb}_{0.2}$ QWFETs, where the surface Fermi level

sweeps below the midgap of GaSb towards the valence band (Fig. 2b). From XPS measurements we estimate the valence and conduction band offsets to be 3.4eV and 2.4eV respectively, sufficient for gate leakage suppression (Figs. 4a,b). Fig. 3 shows the schematic of the $\text{InAs}_{0.8}\text{Sb}_{0.2}$ MOS QWFET with GaSb and Al_2O_3 dielectric which forms a composite gate stack on top of the QW. Fig. 5 shows the energy band diagram of the $\text{InAs}_{0.8}\text{Sb}_{0.2}$ QW structure with the composite Al_2O_3 -GaSb gate stack using Schrodinger-Poisson simulation, indicating strong electron confinement in the $\text{InAs}_{0.8}\text{Sb}_{0.2}$ QW. Figs. 6a,b show the TEM micrographs of the $\text{InAs}_{0.8}\text{Sb}_{0.2}$ QWFET stack grown on GaAs by MBE and the active device layers. Hall measurements were performed on the device layers by varying the temperature from 4K-300K (Figs. 7a,b). Table 1 shows the percentage contribution to $1/\mu$ from individual scattering mechanisms at 300K. Near the room temperature, intra and inter sub-band acoustic deformation potential (ADP) scattering and interface defect scattering⁵ dominate. Shubnikov-de Haas (SdH) oscillations (Fig. 8a) are observed at low temperature (2-15K) and high magnetic fields (0-9Tesla) confirming excellent channel and interface quality. An effective mass of $0.043m_0$ is extracted from the temperature dependence of the amplitude of SdH oscillations, which is lower than $0.05m_0$ reported for InAs QW due to quantization and band non-parabolicity⁶. FFT of SdH oscillations vs. $1/B$ at 2K (Fig. 8b) shows single peak confirming majority carrier transport in the first subband of the QW at $n_s = 2 \times 10^{12}/\text{cm}^2$ and no parallel conduction.

Device Characterization

Figs. 9a,b show the top view SEM and cross-section TEM of the $\text{InAs}_{0.8}\text{Sb}_{0.2}$ MOS QWFET with 100nm physical gate length (L_g) and the composite Al_2O_3 -GaSb gate stack. Pd/Pt/Au metal stack was alloyed to form embedded contacts making direct contact with the QW (Fig.10). Circular TLM measurements before and after PEALD Al_2O_3 deposition are shown in Fig. 11. Figs. 12a,b show the split C- V_G characteristics of $\text{InAs}_{0.8}\text{Sb}_{0.2}$ MOS-QWFET for 4.4nm and 3.3nm physically thick Al_2O_3 and the frequency dispersion characteristics. The EOT of the thinner stack is 4.2 nm which includes the 9 nm $\text{Al}_{0.8}\text{In}_{0.2}\text{Sb}$ barrier and 12 nm $\text{InAs}_{0.8}\text{Sb}_{0.2}$ QW capacitance. Conductance vs frequency contour plot (Figs. 13a,b) shows positive slope with V_G indicating electron capture/emission process. This could be due to

Report Documentation Page				Form Approved OMB No. 0704-0188	
Public reporting burden for the collection of information is estimated to average 1 hour per response, including the time for reviewing instructions, searching existing data sources, gathering and maintaining the data needed, and completing and reviewing the collection of information. Send comments regarding this burden estimate or any other aspect of this collection of information, including suggestions for reducing this burden, to Washington Headquarters Services, Directorate for Information Operations and Reports, 1215 Jefferson Davis Highway, Suite 1204, Arlington VA 22202-4302. Respondents should be aware that notwithstanding any other provision of law, no person shall be subject to a penalty for failing to comply with a collection of information if it does not display a currently valid OMB control number.					
1. REPORT DATE DEC 2010		2. REPORT TYPE		3. DATES COVERED 00-00-2010 to 00-00-2010	
4. TITLE AND SUBTITLE Advanced Composite High-γ Gate Stack for Mixed Anion Arsenide-Antimonide Quantum Well Transistors				5a. CONTRACT NUMBER	
				5b. GRANT NUMBER	
				5c. PROGRAM ELEMENT NUMBER	
6. AUTHOR(S)				5d. PROJECT NUMBER	
				5e. TASK NUMBER	
				5f. WORK UNIT NUMBER	
7. PERFORMING ORGANIZATION NAME(S) AND ADDRESS(ES) Naval Research Laboratory, 4555 Overlook Avenue SW, Washington, DC, 20375				8. PERFORMING ORGANIZATION REPORT NUMBER	
9. SPONSORING/MONITORING AGENCY NAME(S) AND ADDRESS(ES)				10. SPONSOR/MONITOR'S ACRONYM(S)	
				11. SPONSOR/MONITOR'S REPORT NUMBER(S)	
12. DISTRIBUTION/AVAILABILITY STATEMENT Approved for public release; distribution unlimited					
13. SUPPLEMENTARY NOTES Proceeding of the 2010 IEEE International Electron Devices Meeting (IEDM), 6-8 Dec 2010 in San Francisco, CA					
14. ABSTRACT This paper demonstrates the integration of a composite high-γ gate stack (3.3 nm Al₂O₃-1.0 nm GaSb) with a mixed anion InAs_{0.8}Sb_{0.2} quantum-well field effect transistor (QWFET). The composite gate stack achieves (i) EOT of 4.2 nm with <10⁻⁷ A/cm² gate leakage (ii) low Dit interface (~1x10¹² /cm²/eV) (iii) high drift μ of 3,900-5,060 cm²/V-s at NS of 5x10¹¹-3x10¹²/cm². The InAs_{0.8}Sb_{0.2} MOS-QWFETs with composite gate stack exhibit extrinsic (intrinsic) gm of 334 (502) μS/μm and drive current of 380 μA/μm at VDS = 0.5V for Lg=1μm.					
15. SUBJECT TERMS					
16. SECURITY CLASSIFICATION OF:			17. LIMITATION OF ABSTRACT Same as Report (SAR)	18. NUMBER OF PAGES 4	19a. NAME OF RESPONSIBLE PERSON
a. REPORT unclassified	b. ABSTRACT unclassified	c. THIS PAGE unclassified			

the traps at the oxide-GaSb interface. **Fig. 14** plots J_{OX} vs V_G showing less than 10^{-7} A/cm² of gate leakage in InAs_{0.8}Sb_{0.2} MOS-QWFET. Room temperature drift mobility values of 3,900-5,060 cm²/V-s at carrier concentrations of 5×10^{11} - 3×10^{12} /cm² are extracted from split C- V_G data (**Fig. 15**). **Figs. 16-17** show the drain current (I_D) vs. gate voltage (V_G) of InAs_{0.8}Sb_{0.2} MOS-QWFET for various L_G and L_{SIDE} . Parasitic access resistance limits the achievable on-current in the fabricated devices. For the shortest L_{SIDE} of 0.25 μ m and $L_G = 1 \mu$ m, the best extrinsic g_m and I_D at 300K are 334 μ S/ μ m and 380 μ A/ μ m, and at 77K are 630 μ S/ μ m and 411 μ A/ μ m at $V_{DS} = 0.5$ V. Peak intrinsic g_m increases to 502 μ S/ μ m (1,070 μ S/ μ m) at 300K (77K) (**Fig. 19**). **Fig. 18** shows the output characteristics of the device at 300K and 77K for $L_G = 1 \mu$ m and $L_{SIDE} = 0.25 \mu$ m. The high off-state leakage of InAs_{0.8}Sb_{0.2} MOS-QWFET at 300K is likely due to the hole accumulation in the Al_{0.8}In_{0.2}Sb barrier layer screening the gate potential as well as the generation of holes due to impact ionization. The source side effective injection velocity, V_{eff} , is extracted as a function of $V_{GSi} - V_T$ at 77K for InAs_{0.8}Sb_{0.2} MOS-QWFET (**Fig. 20**). The highest V_{eff} obtained is 1.4×10^7 cm/s, one of the highest values ever reported for III-V MOS QWFETs.

Conclusions

An advanced composite high- κ gate stack (3.3nm Al₂O₃-1.0nm GaSb) is successfully integrated in the mixed anion InAs_{0.8}Sb_{0.2} QWFET with low EOT (4.2nm), negligible J_{OX} (10^{-7} A/cm²) and high drift μ (3,900-5,060 cm²/V-s). The InAs_{0.8}Sb_{0.2} MOS-QWFETs with $L_g = 1 \mu$ m exhibit intrinsic transconductance of 502 μ S/ μ m and 1,070 μ S/ μ m and drive currents of 380 μ A/ μ m and 411 μ A/ μ m at room temperature and 77K, respectively, all at $V_{DS} = 0.5$ V.

References

- ¹J. B. Boos et al., *IEICE Trans.* vol. E85-A/B/C/D, no. 7, July (2008)
- ²M. Radosavljevic et al., *IEDM Tech. Dig.* pp. 319, Dec (2009)
- ³B. P. Tinkham, et al., *J. Vac. Sci. Technol.* B 23, pp. 1441 (2005)
- ⁴A. Ali et al., *Dev. Res. Conf.* June (2010)
- ⁵C. Nguyen et al., *Appl. Phys. Lett.* pp. 1854 (1992)
- ⁶D. Jin et al., *IEDM Tech Dig.*, pp. 495 (2009)

Acknowledgement

We acknowledge financial support from DARPA/SRC sponsored MARCO-MSD Center.

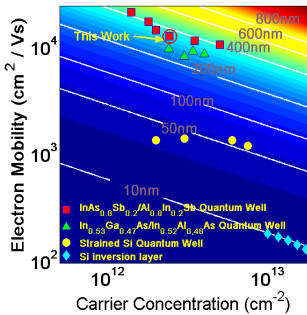


Fig. 1 Electron mobility vs carrier concentration overlaid on a contour map of ballistic mean free path

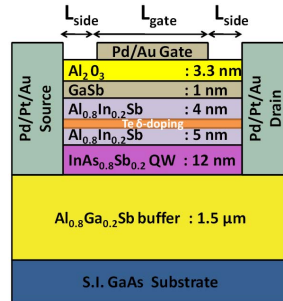


Fig. 3 Schematic of InAs_{0.8}Sb_{0.2} MOS QWFET on GaAs substrate with 1nm GaSb and 3.3nm PEALD Al₂O₃ dielectric which forms a composite Al₂O₃-GaSb gate stack on top of QW

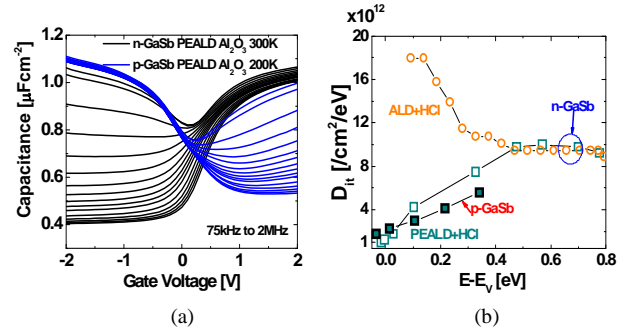


Fig. 2 (a) Unpinned C-V characteristics of n-type and p-type GaSb (100) MOS capacitors with PEALD Al₂O₃ (b) D_{it} of $1-3 \times 10^{12}$ /cm²/eV near E_v achieved with PEALD Al₂O₃ samples

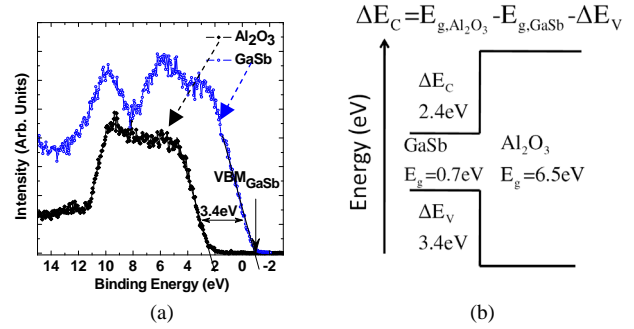


Fig. 4 (a) Measured energy difference between the valence band spectra of Al₂O₃ and GaSb (100) gives valence band offset of 3.4eV (b) Valence and conduction band offsets derived from XPS analysis

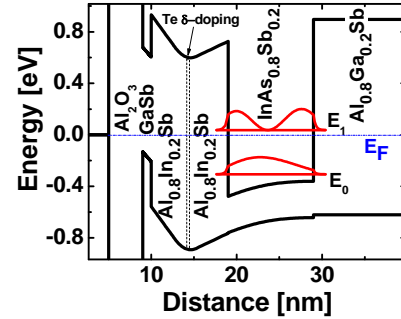


Fig. 5 Band diagram of InAs_{0.8}Sb_{0.2} MOS QWFET with 1nm GaSb and 3.3nm PEALD Al₂O₃ dielectric from Schrodinger-Poisson simulation

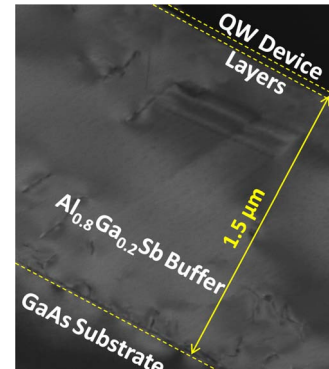


Fig. 6 (a) Cross-sectional TEM micrograph of InAs_{0.8}Sb_{0.2} QW stack on GaAs substrate using Al_{0.8}Ga_{0.2}Sb relaxed buffer layer

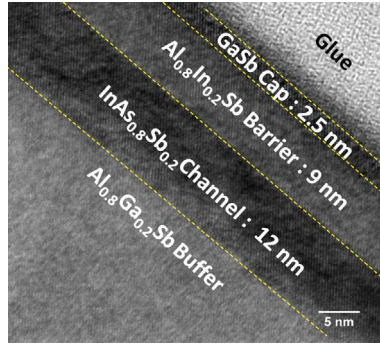


Fig. 6 (b) High resolution TEM micrograph of InAs_{0.8}Sb_{0.2} QW stack with as deposited 2.5nm GaSb (surface preparation prior to oxide deposition reduces GaSb thickness to 1nm)

	% contribution to $1/\mu$ at 300K
Interface Charge	50%
ADP Scattering	23%
Remote Ionized Impurity Scattering	13%
Alloy Scattering	8%
Polar Optical Phonon Scattering	6%

Table 1 Percentage contribution to $1/\mu_{\text{Total}}$ at 300K

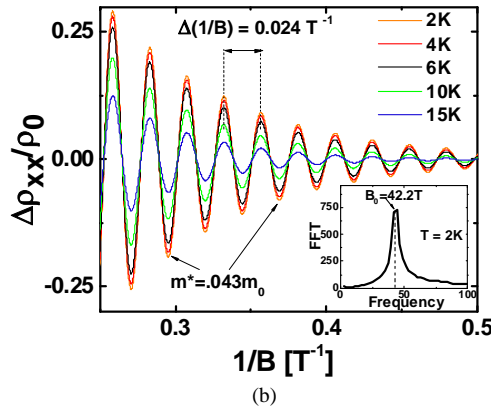
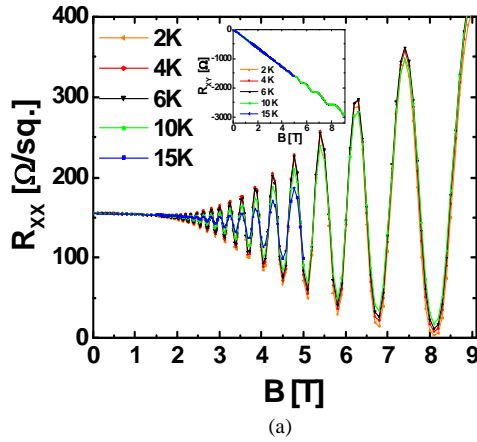


Fig. 8 (a) Shubnikov-de Haas (SdH) oscillations in the sheet resistance. Temperature dependence of the amplitude of these oscillations is used to calculate m^* (b) FFT of SdH oscillations vs. $1/B$ at 2K (inset) shows single peak confirming majority carrier transport in the first subband of the QW at $n_s = 2 \times 10^{12}/\text{cm}^2$ and no parallel conduction

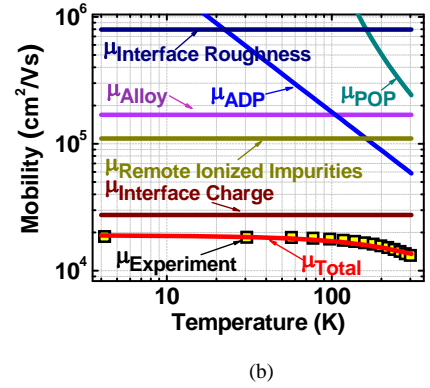
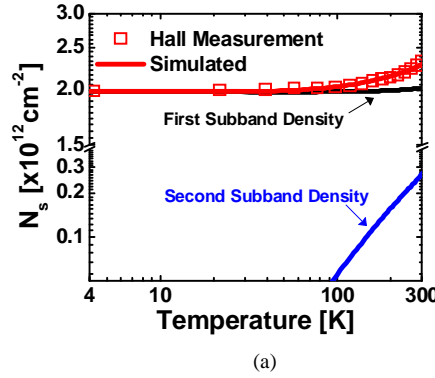


Fig. 7 (a) Carrier density (N_s), and (b) Hall mobility vs temperature for InAs_{0.8}Sb_{0.2} QW

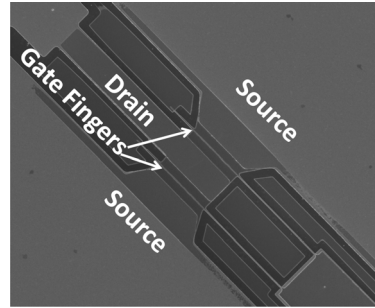


Fig. 9 (a) Top view SEM of InAs_{0.8}Sb_{0.2} QWFET with composite Al₂O₃-GaSb gate stack on top of the QW

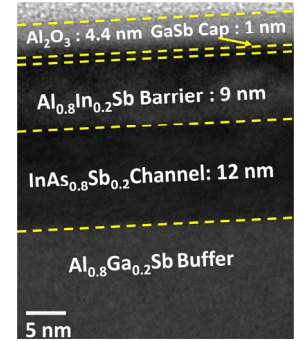


Fig. 9 (b) Cross-section TEM of InAs_{0.8}Sb_{0.2} MOS QWFET with 1.0nm GaSb-4.4nm PEALD Al₂O₃ composite gate stack on top of the QW

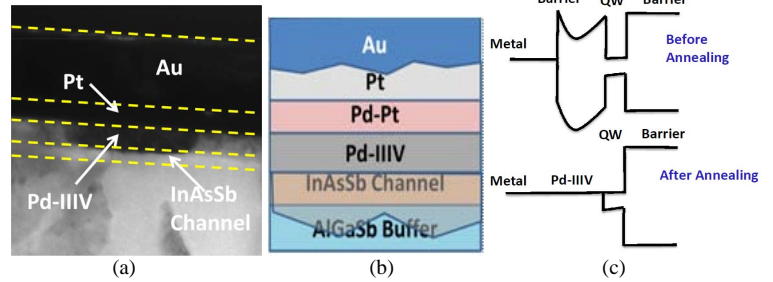


Fig. 10 (a) Cross-section TEM of InAs_{0.8}Sb_{0.2} MOS QWFET under the alloyed embedded contact directly contacting the InAs_{0.8}Sb_{0.2} channel (b) Schematic cross-section of the region underneath the ohmic contact (c) Band diagram explaining the embedded ohmic contact formation

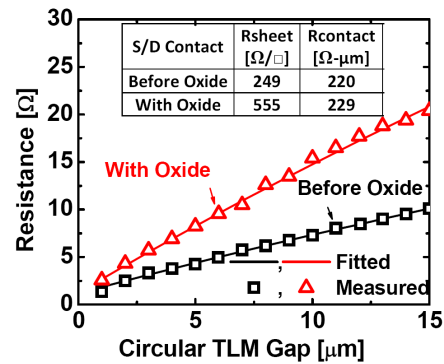


Fig. 11 Circular TLM measurements before and after PEALD Al₂O₃ deposition

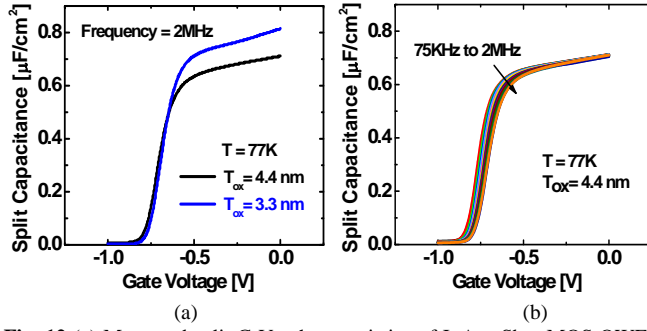


Fig. 12 (a) Measured split C-V_G characteristics of InAs_{0.8}Sb_{0.2} MOS QWFET with various composite gate stack thickness (b) Frequency dispersion of the C-V_G characteristics of InAs_{0.8}Sb_{0.2} MOS QWFET

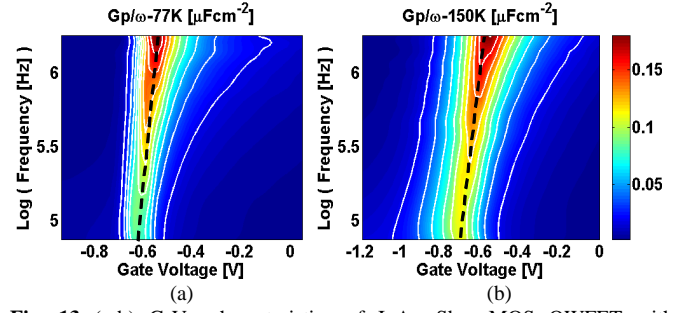


Fig. 13 (a-b) G-V_G characteristics of InAs_{0.8}Sb_{0.2} MOS QWFET with composite gate stack; peak conductance trace reflects Fermi level movement in the InAs_{0.8}Sb_{0.2} QW

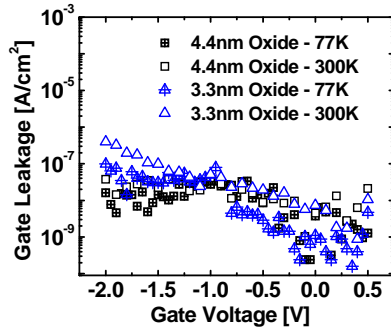


Fig. 14 J_{OX} vs V_G showing lower than 10⁻⁷ A/cm² of gate leakage in InAs_{0.8}Sb_{0.2} MOS-QWFET

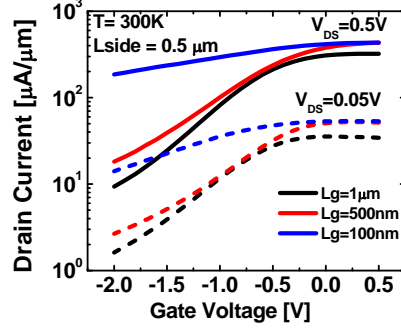


Fig. 16 L_G scaling: Drain current (I_D) vs. gate voltage (V_G) of InAs_{0.8}Sb_{0.2} MOS-QWFET with L_G = 1 μm, 500nm, 100nm and Al₂O₃-GaSb composite stack (EOT = 4.2nm) at 300K and 77K at V_{DS} = 0.5V, 50mV (L_{SIDE} = 0.5 μm)

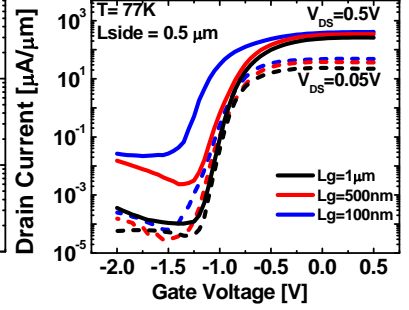


Fig. 17 L_{SIDE} scaling: I_D vs. V_G of L_G = 100nm InAs_{0.8}Sb_{0.2} MOS-QWFET with composite stack at 77K at V_{DS} = 0.5V with L_{SIDE} = 0.5, 1 and 2 μm

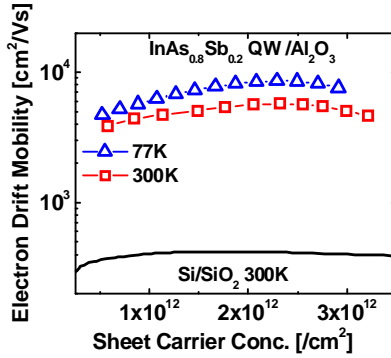


Fig. 15 Drift μ vs N_s at 77K and 300K in InAs_{0.8}Sb_{0.2} MOS QWFET from split C-V_G measurements

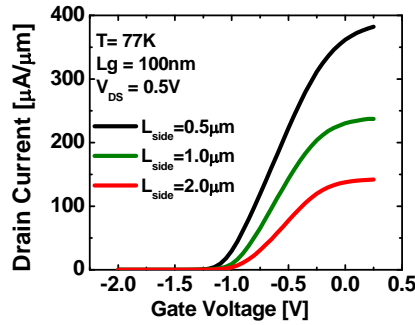


Fig. 18 Output Characteristics: I_D vs. V_{DS} of InAs_{0.8}Sb_{0.2} MOS-QWFET with L_G = 1 μm, L_{SIDE} = 0.25 μm and Al₂O₃-GaSb composite stack (EOT = 4.2nm) at 300K and 77K

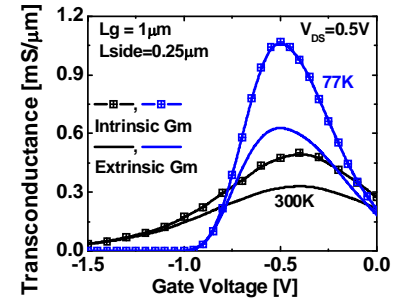


Fig. 19 Transconductance (g_m) characteristics of InAs_{0.8}Sb_{0.2} MOS-QWFET with L_G = 1 μm, L_{SIDE} = 0.25 μm and Al₂O₃-GaSb composite stack (EOT = 4.2nm) at 300K and 77K. Intrinsic peak g_m is 502 μS/μm and 1070 μS/μm at 300K and 77K, respectively

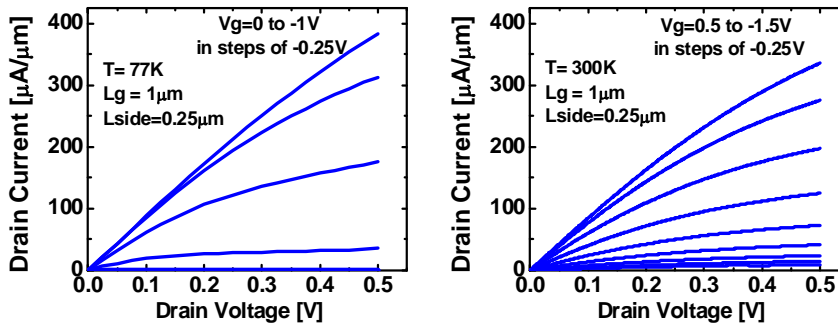


Fig. 20 Extracted effective injection velocity, V_{eff}, as a function of V_{GSI}-V_T using the charge obtained from split C-V_G measurements and I_{D,SAT} vs V_{GSI}-V_T. The V_T from split C-V_G is matched to the V_{T,SAT} from I_{D,SAT} vs V_{GSI}-V_T to obtain V_{eff}